Inorg. Chem. **2008**, *47*, 7474−7482

In Situ Spectroscopy and Spectroelectrochemistry of Uranium in High-Temperature Alkali Chloride Molten Salts

Ilya B. Polovov,*,† Vladimir A. Volkovich,† John M. Charnock,‡ Brett Kralj,§ Robert G. Lewin,§ Hajime Kinoshita,∥,⊥ Iain May,∥,# and Clint A. Sharrad*,∥

Department of Rare Metals, Ural State Technical University−UPI, Ekaterinburg 62002, Russia, CCLRC Daresbury Laboratory, Daresbury, Warrington, Cheshire WA4 4AD, U.K., Nexia Solutions, B13022, Sellafield, Seascale, Cumbria CA20 1PG, U.K., and Centre for Radiochemistry Research, School of Chemistry, The University of Manchester, Oxford Road, Manchester M13 9PL, U.K.

Received July 16, 2007

Soluble uranium chloride species, in the oxidation states of III+, IV+, V+, and VI+, have been chemically generated in high-temperature alkali chloride melts. These reactions were monitored by in situ electronic absorption spectroscopy. In situ X-ray absorption spectroscopy of uranium(VI) in a molten LiCl−KCl eutectic was used to determine the immediate coordination environment about the uranium. The dominant species in the melt was $[UO_2Cl_4]^{2-}$. Further analysis of the extended X-ray absorption fine structure data and Raman spectroscopy of the melts quenched back to room temperature indicated the possibility of ordering beyond the first coordination sphere of $[UO_2Cl_4]^{2-}$. The electrolytic generation of uranium(III) in a molten LiCl−KCl eutectic was also investigated. Anodic dissolution of uranium metal was found to be more efficient at producing uranium(III) in high-temperature melts than the cathodic reduction of uranium(IV). These high-temperature electrolytic processes were studied by in situ electronic absorption spectroelectrochemistry, and we have also developed in situ X-ray absorption spectroelectrochemistry techniques to probe both the uranium oxidation state and the uranium coordination environment in these melts.

Introduction

High-temperature molten salt media have been used in separation processes by the nuclear industry for over half a century.[1] Electrorefining of plutonium in molten salts is undertaken for military applications, while the electrochemical separation of uranium from spent nuclear fuel can be linked to the development of molten salt compatible nuclear reactors. Chloride-based salts are preferred in pyrochemical nuclear applications because of their radiolytic stability and their capacity of facilitating the conversion of highly insoluble oxide mixtures into a soluble form. The two most industrially advanced processes are based on NaCl−KCl and LiCl−KCl melts,[2] with research efforts now focused on the next generation of pyrochemical processes for actinide separations.[3] An increased understanding of actinide chemical speciation and redox processes would complement this applied research, but the harsh chemical environment afforded by the high-temperature corrosive salts renders in situ studies extremely challenging.

* To whom correspondence should be addressed. E-mail: polovov@dpt.ustu.ru (I.B.P.), clint.a.sharrad@manchester.ac.uk (C.A.S.). Tel: +7 343 375 4813 (I.B.P.), +44 161 275 4657 (C.A.S.). Fax: +7 343 374 5491 (I.B.P.), +44 161 275 4598 (C.A.S.).

† Ural State Technical University−UPI.

‡ CCLRC Daresbury Laboratory.

§ Nexia Solutions.

⊥ Current address: Department of Engineering, Sir Robert Hadfield Building, Mapping Street, The University of Sheffield, Sheffield S1 3JD, U.K.

∥ The University of Manchester.

Current address: Chemistry−Inorganic Isotope and Actinide Chemistry, Los Alamos National Laboratory, Los Alamos, NM 87545.

(1) (a) Weinberg, A. *Nucleonics* **1957**, *15*, 64. (b) Lovering, D. G., Ed. *Molten Salt Technology*; Plenum: New York, 1982; and references cited therein. (c) Gale, R. J., Lovering, D. G., Eds. *Molten Salt Techniques*; Plenum: New York, 1984. (d) Lambertin, D.; Ched'homme, S.; Bourges, G.; Sanchez, S.; Picard, G. S. *J. Nucl. Mater.* **2005**, *341*, 131. (e) Ackerman, J. P. *Ind. Eng. Chem. Res.* **1991**, *30*, 141.

(2) (a) Laidler, J. J.; Battles, J. E.; Miller, W. E.; Ackerman, J. P.; Carls, E. L. *Prog. Nucl. Energy* **1997**, *31*, 131. (b) Bychkov, A. V.; Vavilov, S. K.; Porodnov, P. T.; Skiba, O. V.; Popkov, G. P.; Pravdin, A. K. *Molten Salt Forum* **1998**, 525.

(3) For example, see: (a) Serp, J.; Konings, R. J. M.; Malmbreck, R.; Rebizant, J.; Schlepper, C.; Glatz, J.-P. *J. Electroanal. Chem.* **2004**, *561*, 143. (b) Uozumi, K.; Iizuka, M.; Kato, T.; Inoue, T.; Shirai, O.; Iwai, T.; Arai, Y. *J. Nucl. Mater.* **2004**, *325*, 34. (c) Serrano, K.; Taxil, P. *J. Appl. Electrochem.* **1999**, *29*, 497.

10.1021/ic701415z CCC: $40.75
Published on Web 07/30/2008

Electronic absorption spectroscopy (EAS) has been shown to be an effective in situ method of probing the uranium oxidation state in high-temperature melts.[4] In some examples, this has been extended to include aspects of coordination.[5] The techniques of Raman and NMR spectroscopies have been used as in situ methods for metal speciation in high-temperature systems.[6] Okamoto et al. used X-ray absorption spectroscopy (XAS) to study the in situ speciation of uranium(III) in LiCl−KCl melts (550 °C), confirming that the first coordination sphere is filled with Cl^- ligands.[7] We have subsequently made extensive use of extended X-ray absorption fine structure (EXAFS) measurements, combined with EAS studies, to investigate the local environment around uranium in high-temperature melts in all four different oxidation states (III, IV, V, and VI).[8–13]

Of more industrial relevance would be an increased understanding of speciation with respect to electrochemical processes. The in situ analysis of electrolytically generated species in pyrochemical processes has previously been limited to EAS detection.[14,15] Nagai et al. have investigated the $\{UO_2\}^{2+}/\{UO_2\}^{+}$ redox equilibrium in a molten CsCl−NaCl eutectic using EAS spectroelectrochemistry.[14] Previously, XAS spectroelectrochemical investigations of actinides in room temperature solutions had been performed in thin-layer or poly(tetrafluoroethylene) electrochemical cells.[16,17] However, these techniques are not readily applicable to high-temperature investigations.

We now report a major extension to our uranium studies in high-temperature melts. The effectiveness of XAS in combination with EAS for the in situ determination of the redox speciation and uranium coordination environment has been investigated. The $\{UO_2\}^{2+}$ system has been studied in more detail by in situ XAS measurements in different salts and at different temperatures. Raman spectroscopy of uranyl-containing chloride melts after quenching back to room temperature has also been conducted. These additional experiments were designed to probe further the possibility of long-range ordering that has been observed previously in uranium(IV) systems.[11] Finally, we have developed a spectroelectrochemical capability that has been used to determine the most effective method of generating pure uranium(III), the oxidation state of most relevance to pyrochemical fuel processing operations.[2,3]

Experimental Section

Caution! *Both natural (0.72 wt % ^{235}U) and depleted uranium (0.20 wt % ^{235}U) were used during the course of these experiments. As well as the radioactive hazards associated with ^{238}U and ^{235}U, uranium is a toxic metal and care should be taken with all manipulations.*

Instrumentation. An Instrom furnace, capable of reaching 1100 °C, was used to prepare and to study samples at high temperature. The furnace was adapted to include quartz windows to allow for high-temperature EAS measurements and beryllium windows for XAS experiments.

UV−visible−near-IR spectroscopic measurements were conducted using an Avantes Avaspec-2048-2 spectrometer using an Avalight DH-S deuterium−halogen light source. For high-temperature measurements, fiber-optic cables were utilized for both detection and incident beams. An Avalight collimating lens was attached to the end of the fiber-optic cable for the incident beam. Diffuse-reflectance spectra of powdered quenched-melt samples were obtained using a reflectance fiber-optic probe. MgO was used for baseline measurements. Hygroscopic and air-sensitive quenched melts were analyzed inside a drybox under an argon atmosphere. Band analysis of all UV−vis−near-IR data was conducted using *PeakFit*.[18]

Raman spectra of quenched melts were obtained using a Bruker Equinox 55/Bruker FRA 106/5 with a coherent 500 mW laser. Hygroscopic and air-sensitive melts were sealed inside a glass capillary under an argon atmosphere.

Uranium concentrations in quenched melts were measured using a Fisons Horizon Elemental Analysis ICP-OED spectrometer. Oxidimetric analyses were conducted using previously described methods.[10,19] The average oxidation state values determined have an error of ±5%.

All electrochemistry procedures used a Solartron 1287 potentiostat connected to the electrodes to control the current or potential.

(4) For example, see: (a) Silcox, N. W.; Haendler, H. M. *J. Phys. Chem.* **1960**, *64*, 303. (b) Young, J. P. *Inorg. Chem.* **1967**, *6*, 1486. (c) Young, J. P.; White, J. C. *Anal. Chem.* **1960**, *32*, 799. (d) Morrey, J. R.; Voiland, E. E. *Spectrochim. Acta* **1962**, *18*, 1175. (e) Morrey, J. R. *Inorg. Chem.* **1963**, *2*, 163. (f) Dai, S.; Toth, L. M.; Del Cul, G. D.; Metcalf, D. H. *J. Phys. Chem.* **1996**, *100*, 220. (g) Adams, M. D.; Wenz, D. A.; Steunenberg, R. K. *J. Phys. Chem.* **1963**, *67*, 1939. (h) Wenz, D. A.; Adams, M. D.; Steunenberg, R. K. *Inorg. Chem.* **1964**, *3*, 989.

(5) (a) Volkovich, V. A.; Bhatt, A. I.; May, I.; Griffiths, T. R.; Thied, R. C. *J. Nucl. Sci. Technol.* **2002**, 595, Supplement 3. (b) Volkovich, V. A.; Griffiths, T. R.; Fray, D. J.; Thied, R. C. *Phys. Chem. Chem. Phys.* **2000**, *2*, 3871. (c) Gruen, D. M.; McBeth, R. L. *J. Inorg. Nucl. Chem.* **1959**, *9*, 290.

(6) (a) Photiadis, G. M.; Papatheodorou, G. N. *J. Chem. Soc., Dalton Trans.* **1999**, 3541. (b) Schellkes, E.; Hong, X.; Holz, M.; Huniar, U.; Ahlrichsand, R.; Freyland, W. *Phys. Chem. Chem. Phys.* **2003**, *5*, 5836. (c) Papatheodorou, G. N. *Inorg. Chem. Nucl. Lett.* **1975**, *11*, 483. (d) Rollet, A.-L.; Bessada, C.; Rakhmatoulline, A.; Auger, Y.; Melin, P.; Gailhanou, M.; Thiaudière, C. R. *Chimie* **2004**, *7*, 1135.

(7) Okamoto, Y.; Akabori, M.; Itoh, A.; Ogawa, T. *J. Nucl. Sci. Technol.* **2002**, 638, Supplement 3.

(8) Volkovich, V. A.; May, I.; Charnock, J. M. *Rasplavy* **2004**, *2*, 76.

(9) Volkovich, V. A.; May, I.; Griffiths, T. R.; Charnock, J. M.; Bhatt, A. I.; Lewin, B. *J. Nucl. Mater.* **2005**, *344*, 100.

(10) Volkovich, V. A.; May, I.; Bhatt, A. I.; Griffiths, T. R.; Charnock, J. M.; Lewin, B. In *Proceedings of the International Symposium on Ionic Liquids*; Øye, H. A., Jagtøyen, A., Eds.; Carry le Rouet, The Norwegian University of Science and Technology: Trondheim, Norway, 2003; p 253.

(11) Bhatt, A. I.; Kerdaniel, E. F.; Kinoshita, H.; Livens, F. R.; May, I.; Polovov, I. B.; Sharrad, C. A.; Volkovich, V. A.; Charnock, J. M.; Lewin, R. G. *Inorg. Chem.* **2005**, *42*, 2.

(12) Volkovich, V. A.; May, I.; Sharrad, C. A.; Kinoshita, H.; Polovov, I. B.; Bhatt, A. I.; Charnock, J. M.; Griffiths T. R.; Lewin, R. G. In *Recent Advances in Actinide Science*; Alvarez, R., Bryan, N. D. , May, I., Eds.; Royal Society of Chemistry: London, 2006; p 485.

(13) Sharrad, C. A.; May, I.; Kinoshita, H.; Bhatt, A. I.; Volkovich, V. A.; Polovov, I. B.; Charnock, J. M.; Lewin, R. G. In *Recent Advances in Actinide Science*; Alvarez, R., Bryan, N. D., May, I., Eds.; Royal Society of Chemistry: London, 2006; p 796.

(14) Nagai, T.; Fujii, T.; Shirai, O.; Yamana, H. *J. Nucl. Sci. Technol.* **2004**, *41*, 690.

(15) Smirnov, M. V.; Potapov, A. M. *Electrochim. Acta* **1994**, *39*, 143.

(16) Sharpe, L. R.; Heineman, W. R.; Elder, R. C. *Chem. Rev.* **1990**, *90*, 705.

(17) Hennig, C.; Tutschku, J.; Rossberg, A.; Bernard, G.; Scheinost, A. C. *Inorg. Chem.* **2005**, *44*, 6655.

(18) *PeakFit*, version 4.11; Systat Software Inc.: San Jose, CA, 2002.

(19) Vogel, A. I. *A Textbook of Quantitative Inorganic Analysis*, 3rd ed.; Longmans: London, 1961.

Sample Preparation. Samples of uranium metal, UCl_4, UO_2, and UO_3, were obtained from The Centre for Radiochemistry Research (Manchester, U.K.) isotope stocks and/or Nexia Solutions (Sellafield, U.K.). Uranium metal was treated in a dilute HNO_3 solution and washed with acetone before use. A LiCl−KCl eutectic (99.9%, Aldrich), a NaCl−CsCl eutectic (99.9%, Aldrich), LiCl (99+%, Aldrich), NaCl (99+%, Aldrich), KCl (99.8%, Fisher Scientific), and CsCl (99+%, Alfa Aesar) were used as supplied. NaCl−KCl (1:1, mol/mol) was prepared by melting equimolar mixtures of NaCl and KCl in vacuo at 800 °C and then quenched under an argon atmosphere.

Samples containing a uranium material (UCl_4, UO_2, UO_3, and U metal) and an alkali chloride salt were placed in a specially made quartz cell and sealed with a rubber stopper under an argon atmosphere. The cell consisted of a quartz optical cell of 1 cm path length, allowing for EAS measurements, attached to a quartz cylinder that had side arms for gas/vacuum inlets. The sample was melted in vacuo (>400 °C). The cell was then brought back to atmospheric pressure under an argon atmosphere. For chlorination experiments, HCl or Cl_2 was sparged through the melt using a silica tube pierced through the rubber stopper at the top of the cell. At the conclusion of chlorination, the tube was raised above the melt and the cell purged with argon for several minutes. The sample was then quenched by extracting the melt into the silica tube.

General XAS Measurements. Previously prepared quenched samples were held in an elongated T-shaped silica cell (to account for the beam geometry) with a wall thickness of 1 mm and a path length of 2 or 3 mm, heated in an optical furnace with two beryllium windows (at 180° in transmission mode and 90° in fluorescence mode). Quenched-melt samples (doubly contained in polyethylene bags) were also analyzed at room temperature.

U L_{III}-edge XAS was conducted at the CCLRC Daresbury Radiation Source in the fluorescence mode at station 16.5 (spectroelectrochemical experiments) and in the transmission mode at station 9.3 (all other samples), operating at a typical beam current of 150 mA and an energy of 2 GeV. The radiation was passed through a monochromator consisting of a Si(220) double crystal and detuned to 50% of the maximum intensity to minimize harmonic generation. The monochromator was calibrated using the K edge of a zirconium foil, taking the first inflection point in the Zr edge as 17 999.4 eV. The fluorescence detector consisted of an array of 30 high-purity germanium windows mounted in a common cryostat and using high-count-rate XPRESS signal processing electronics. Cathodic reduction data were collected to an E_{max} of 18.0 keV, while anodic dissolution data were collected using fast EXAFS spectroscopy to an E_{max} of 17.7 keV. The spectra were summed, calibrated, and background-subtracted using the Daresbury Laboratory programs *EXCALIB*, *EXBACK*, and *EXSPLINE*. The spectra were simulated using the *EXCURV98* program[20] by fitting model coordination environments.

In Situ EAS Spectroelectrochemistry. Anodic dissolution experiments in a molten LiCl−KCl eutectic (450 °C) were conducted using a uranium rod (3 g) attached to a molybdenum wire. Cathodic reduction of $[UCl_6]^{2-}$ (0.01 wt % U), formed by the reaction of UCl_4 with HCl, in a LiCl−KCl eutectic (450 °C) was performed using a platinum wire working electrode covered with a silica sheath. A chlorine/chloride electrode acted as both the counter and reference electrodes for both of these experiments. The sample was melted under argon in the same cell as that described for EAS experiments. The electrodes were then lowered into the melt, and chronopotentiometry was performed (15 mA cathodic reduction and 50 mA anodic dissolution). Quenched samples were obtained at the conclusion of these experiments and analyzed.

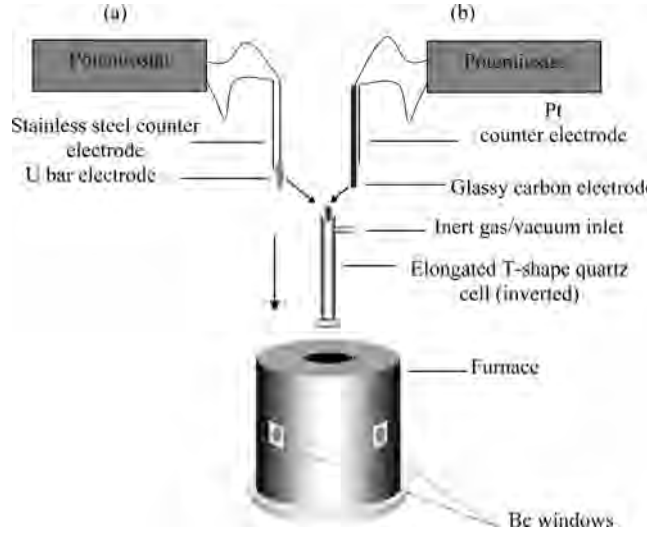

Figure 1. Schematic diagram of the experimental apparatus used for in situ EXAFS spectroelectrochemistry on uranium species in high-temperature melts using (a) anodic dissolution and (b) cathodic reduction processes.

In Situ XAS Spectroelectrochemistry. Anodic Dissolution. The two-electrode system used consisted of a uranium bar anode (3 g of uranium) attached to a stainless steel wire and a stainless steel wire as the counter electrode (Figure 1a). The electrodes were placed inside the quartz cell containing a pure LiCl−KCl eutectic (5.0 g) and sealed with a rubber stopper at the top of the cell under an argon atmosphere. At the synchrotron facility, the salt was melted in vacuo (450 °C) and brought back to atmospheric pressure by purging with argon. The electrodes were then lowered into the melt, and a current of 50 mA was applied for 30 min, after which time XAS measurements were obtained. At the conclusion of the XAS measurements, the cell was removed from the furnace and the melt allowed to quench.

Cathodic Reduction. As described for the anodic dissolution XAS spectroelectrochemistry experiment using a glassy carbon working electrode and a platinum wire counter electrode covered by an open-ended quartz sheath (Figure 1b), with a prepared melt of UCl_4 (0.2 g) dissolved in a LiCl−KCl eutectic (5.0 g), XAS measurements were obtained for the uranium(IV)-containing melt. The electrodes were then lowered into the melt, and the following potentials were applied: −1.0 V, 0−200 min; −1.8 V, 200−400 min; −2.0 V, 400−600 min. XAS scans were obtained before each change in the potential and at the end of the experiment.

Results and Discussion

EAS. EAS has been used extensively to probe the III+ to VI+ oxidation states of uranium in ionic melts, with ligand-to-metal charge-transfer, 5f−5f, and 5f−6d transitions all observed.[6,13] Figure 2 shows the EAS for chloride complexes of $\{UO_2\}^{2+}$, uranium(IV), and uranium(III) in a LiCl−KCl eutectic at 450 °C, and data analyses of these profiles are presented in Table 1. A reasonably pure uranium(V) stock could only be obtained in LiCl at 750 °C (Table 1 and Figure 2).[10] The spectra can differentiate the four oxidation states, and Beer's law is obeyed for the major f−f transitions in uranium(IV) (see the Supporting Information). However, in most uranium fuel processing operations (e.g., the anodic

(20) Gurman, J.; Binsted, N.; Ross, I. *J. Phys. C* **1984**, *17*, 143.

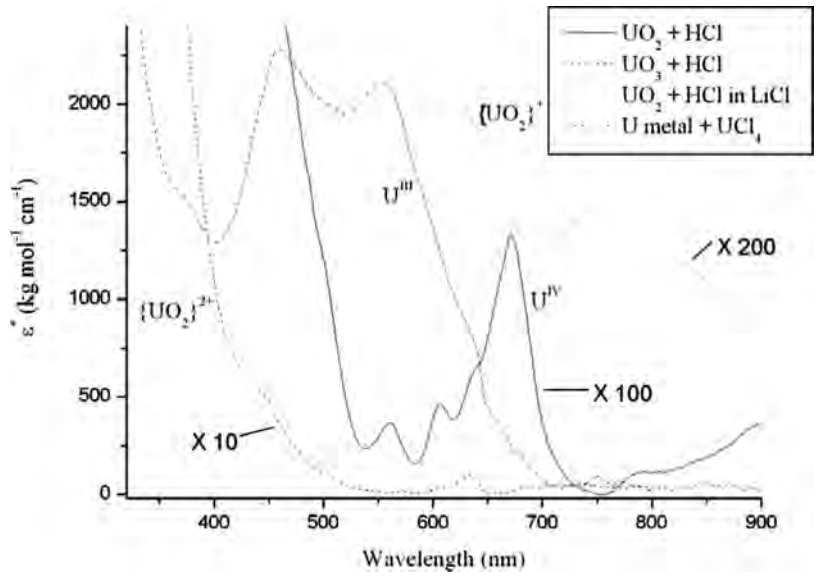

Figure 2. Spectra for various uranium samples in high-temperature alkali chloride melts ($\{UO_2\}^{2+}$, uranium(IV), and uranium(III) in a LiCl−KCl eutectic at 450 °C; uranium(V) in LiCl at 750 °C).

Table 1. Data from Peak-Fitting Analyses[a,18]

sample	λ_{max} (nm)	ϵ^*_{max}[b] (kg mol^{-1} cm^{-1})	fwhm[c] (nm)	R^2[d]
UO_3 exposed to HCl in a LiCl−KCl eutectic at 450 °C	413	46.8	102	0.999 675
UO_2 exposed to HCl in LiCl at 750 °C	612	6.76	102	0.997 679
	768	7.38	277	
UO_2 exposed to HCl in a LiCl−KCl eutectic at 750 °C	549	0.10[e]	48	0.999 013
	608	0.02[e]	16	
	610	0.42[e]	79	
	637	0.05[e]	24	
	670	0.30[e]	50	
	782	0.61[e]	191	
UO_2 exposed to HCl in a LiCl−KCl eutectic at 450 °C	503	4.02	34.3	0.999 735
	560	3.05	30.5	
	605	3.50	22.1	
	634	3.82	27.9	
	671	12.8	41.4	
	791	1.06	27.7	
uranium metal and UCl_4 reacted in a LiCl−KCl eutectic at 450 °C	366	978	66.1	0.999 371
	458	1930	87.6	
	555	1910	106	
	635	316	56.9	

[a] Analysis of fitted peaks centered outside the range of experimental data is not included in this table. [b] Reference 20. [c] fwhm = full width at half-maximum. [d] Reference 18. [e] Absorbance units.

dissolution of uranium metal), uranium(III) will be the dominant species. Laporte-allowed 5f−6d transitions from uranium(III) dominate the visible region of the spectrum with extinction coefficients that are nearly 2 orders of magnitude larger than the next most intense band of the remaining uranium oxidation states.[21] A concentration profile for uranium(III) was difficult to obtain because of the low concentrations required to probe these intense transitions. We also observed the degradation of our quartz cells in the presence of uranium(III), particularly at high uranium concentrations.

Uranyl(VI): Further Spectroscopic Studies. The reaction between UO_3 and HCl in a LiCl−KCl eutectic, followed by melting of the generated sample at 450 °C, results in EXAFS data (Table 2) that can be best fitted with shells for two oxygen (1.75 Å) and four chlorine (2.64 Å) atoms. The U−O and U−Cl bond distances are as expected for the uranyl dioxotetrachloride anion.[22,23]

Increasing the temperature of the melt did not significantly alter the coordination shells (Figure 3 and Table 2). At each temperature, including a third coordination shell of four uranium atoms at ∼4.36 Å in the model provided an improved fit but was not quite sufficient to justify statistically the presence of this shell. There is substantial precedence though from similar uranyl systems generated in aqueous media to suggest that this uranium shell in a molten LiCl−KCl eutectic could indeed exist.[24–26] EXAFS data of uranyl complexes in an aqueous solution have been fitted with long-range [U−U] interactions indicative of dimeric and

(21) Extinction coefficients are calculated in kg mol^{-1} cm^{-1} (i.e., molal) rather than dm^3 mol^{-1} cm^{-1} because of the difficulties involved with obtaining accurate volume measurements for the generated melts.

(22) Danis, J. A.; Lin, M. R.; Scott, B. L.; Eichhorn, B. W.; Runde, W. H. *Inorg. Chem.* **2001**, *40*, 3389.

(23) di Sipio, L.; Tondello, E.; Pelizzi, G.; Ingletto, G.; Montenero, A. *Cryst. Struct. Commun.* **1974**, *3*, 297.

Table 2. EXAFS Data of Uranium(VI) Species

sample	[U] (wt %)	k_{max} (Å^{-1})	occupancy[a]	distance (Å)[b]	$2\sigma^2$ (Å^2)[c]	R
UO_3 exposed to HCl in NaCl−KCl (1:1, mol/mol) at 750 °C	1.40	9.0	U−O(2)	1.77	0.010	27.8
			U−Cl(4)	2.66	0.032	
UO_3 exposed to HCl in a LiCl−KCl eutectic at 450 °C	1.61	9.0	U−O(2)	1.76	0.007	44.3
			U−Cl(4)	2.64	0.024	
UO_3 exposed to HCl in a LiCl−KCl eutectic at 575 °C	1.61	9.0	U−O(2)	1.75	0.004	36.1
			U−Cl (4)	2.61	0.028	
UO_3 exposed to HCl in a LiCl−KCl eutectic at 700 °C	1.61	9.0	U−O(2)	1.75	0.006	34.1
			U−Cl(4)	2.62	0.033	

[a] ±20%. [b] ±0.02 Å. [c] $2\sigma^2$ = Debye−Waller factor.

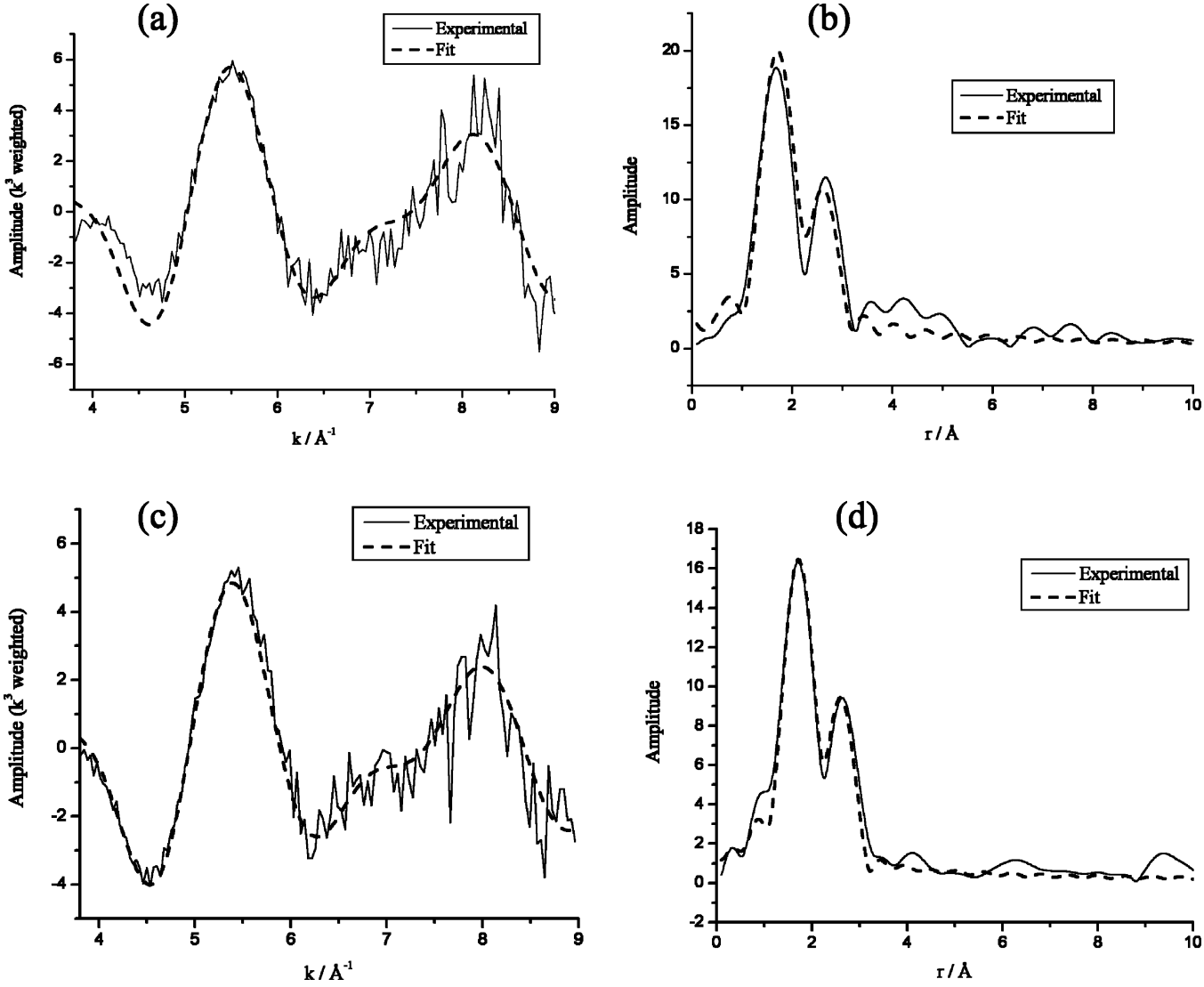

Figure 3. U L_{III}-edge EXAFS spectrum of UO_3 exposed to HCl in a LiCl−KCl eutectic ([U] = 1.40 wt %) at 575 °C (a), with Fourier transformation (b), and in NaCl−KCl (1:1, mol/mol; [U] = 1.61 wt %) at 750 °C (c), with Fourier transformation (d).

trimeric species,[24] and the synthesis of uranyl chloride polymers has been achieved in an aqueous solution using high chloride concentrations where alkali cations also interacted with the $\{UO_2\}^{2+}$ moiety.[25] Solid-state structures of two-dimensional chloro-bridged $\{UO_2\}^{2+}$ tetramers have U−U distances as short as 3.67 Å.[26] It has been shown that oligomeric species of uranium(IV) can be generated in these high-temperature melts.[11] The Debye−Waller factors for all of the U−Cl distances modeled are relatively high, indicating the possibility of a high degree of thermal motion about the Cl shells, and/or there may be several U−Cl distances from a combination of terminal and bridging chloride ligands that contribute to the average shell.

The same reaction undertaken in NaCl−KCl resulted in a data set that could be fitted only by the two oxygen and four chloride ligands of $[UO_2Cl_4]^{2-}$ (see Table 2 and Figure 3). The inclusion of further coordination shells provided no improvement to the fit in this example. Although this suggests that there is no ordered environment passed the chloride shell, it must be remembered that the extent of X-ray absorption from the alkali cation in the melt does increase with the size/weight of the cation,

Table 3. Frequency of Raman-Active Symmetric U−O Stretch of Uranyl Quenched in Various Alkali Chloride Melts

salt (preparation *T*)	$\nu_1(U-O_{symm})$ (cm^{-1})
LiCl (750 °C)	869
NaCl (900 °C)	864
KCl (900 °C)	839
CsCl (900 °C)	833
LiCl−KCl eutectic (450 °C)	840
CsCl−NaCl eutectic (600 °C)	832
NaCl−KCl (1:1, mol/mol; 750 °C)	840

which results in a lower signal-to-noise ratio in the EXAFS profile.

Further evidence that may indicate the consistent formation of higher ordered environments about the $[UO_2Cl_4]^{2-}$ anion in chloride melts comes from the Raman spectra of a range of $\{UO_2\}^{2+}$-containing quenched melts (see Table 3). The $\nu_1(O{=}U{=}O)$ symmetric stretch has often been used as a measure of uranyl bond strength and, in turn, an indirect probe of the surrounding chemical environment.[27] If the melt contains either K^+ or Cs^+, then $\nu_1(O{=}U{=}O)$ lies between 832 and 840 cm^{-1}, while in LiCl and NaCl, $\nu_1(O{=}U{=}O)$ is found at significantly higher energy (869 and 864 cm^{-1}, respectively). Runde et al. have previously shown that alkali cations can interact with both the halides and the "yl" oxygens of uranyl halide species, even though the alkali cations in these examples were coordinated to crown ether molecules.[28] Different modes of alkali cation interactions were found in these species, with the lighter cations tending to favor interactions with the uranyl oxygens while the heavier cations favor the halides. No dependence on the $\nu_1(O{=}U{=}O)$ symmetric stretch was observed with the different binding modes in these examples.[28] However, in alkali chloride melts, there are minimal steric hindrances, allowing the possibility of alkali-metal cations to interact closely with either the uranyl oxygen or the equatorially coordinated chloride anion of $[UO_2Cl_4]^{2-}$. This may have an influence on the $\nu_1(O{=}U{=}O)$ symmetric stretch and ultimately have an impact on long-range order in uranyl-containing melts.

Other Uranium Oxidation States. The reaction of UO_2 with HCl was found consistently to produce brown uranium(V)-containing alkali chloride melts only when molten LiCl at 750 °C was used as the solvent. Chemical analysis of the quenched-melt samples showed that the mean oxidation state of uranium was 5.1 ± 0.1, indicating a predominance of the V+ oxidation state. The same reaction in a molten NaCl−CsCl eutectic and NaCl−KCl (1:1, mol/mol) at various temperatures only produced uranium(IV)-containing melts. The reaction of UO_2 with HCl in a LiCl−KCl eutectic at 450 and 600 °C predominantly produces uranium(IV) species. However, at higher temperatures (750 °C), the formation of mixed uranium(IV) and uranium(V) species in a LiCl−KCl eutectic can be observed (see the Supporting Information). The magnitude of uranium(V) formation relative to uranium(IV) in a very high-temperature (>750 °C) LiCl−KCl eutectic is also seemingly sensitive to the extent of HCl sparging throughout the course of the reaction. It has been noted that low HCl purge rates have a tendency to form uranium(V) species, whereas complete mixing of the salt solution with HCl favors uranium(IV) formation. This may suggest that the formation of uranium(V) or uranium(IV) species from the reaction of UO_2 with HCl in molten chloride salts is dictated by the alkali cation(s). It is known that the electrode potentials for U^{III}/U^0, U^{IV}/U^{III}, and $U^VO_2/U^{IV}O_2$ redox couples are dependent on the average radius of the alkali cation in the melt.[29,30] Other factors that are known to influence uranyl redox properties in room temperature systems include acidity and ionic strength.[31,32] The LiCl−KCl eutectic itself is known to increase in acidity with increasing temperature.[33] The formation of uranium(V) in chloride melts seems to be preferred at high temperature and with small alkali cations.

Uranium(III) species can be formed in alkali chloride media from uranium metal on contact with HCl. This initially produced the distinct dark purple indicative of this oxidation state but is then quickly oxidized to uranium(IV). Uranium(III) can also be formed by the reaction of UCl_4 with uranium metal in a 3:1 molar ratio in high-temperature chloride media, but oxidimetric analysis of the quenched melts gave an average uranium oxidation state of 3.6 ± 0.1, indicating a significant presence of uranium(IV) in the melt, which was not observed by EAS. This is because of the intense uranium(III) d−f transitions swamping the weak uranium(IV) f−f transitions.[34]

In Situ EAS Spectroelectrochemistry. The electoreduction of $[UCl_6]^{2-}$ (initially generated by the dissolution of UCl_4 with HCl) in the LiCl−KCl eutectic at 450 °C brought about an immediate color change from green to deep purple (see Figure 4 for in situ EAS spectra). The bands attributed to

(24) (a) Allen, P. G.; Bucher, J. J.; Clark, D. L.; Edelstein, N. M.; Ekberg, S. A.; Gohdes, J. W.; Hudson, E. A.; Kaltsoyannis, N.; Lukens, W. W.; Neu, M. P.; Palmer, P. D.; Reich, T.; Shuh, D. K.; Tait, C. D.; Zwick, B. D. *Inorg. Chem.* **1995**, *34*, 4797. (b) Allen, P. G.; Shuh, D. K.; Bucher, J. J.; Edelstein, N. M.; Reich, T.; Denecke, M. A.; Nitsche, H. *Inorg. Chem.* **1996**, *35*, 784. (c) Moll, H.; Geipel, G.; Reich, T.; Bernhard, G.; Fanghanel, T.; Grenthe, I. *Radiochim. Acta* **2003**, *91*, 11.

(25) Bean, A. C.; Xu, Y.; Danis, J. A.; Albrecht-Schmitt, T. E.; Scott, B. L.; Runde, W. *Inorg. Chem.* **2002**, *41*, 6775.

(26) (a) Geras'ko, O. A.; Samsonenko, D. G.; Sharanova, A. A.; Virovets, A. V.; Lipkowski, J.; Fedin, V. P. *Russ. Chem. Bull.* **2002**, *51*, 346. (b) Van den Bossche, G.; Spirlet, M. R.; Rebizant, J.; Goffart, J. *Acta Crystallogr. C* **1987**, *43*, 837.

(27) For example, see: (a) Nguyen-Trung, C.; Palmer, D. A.; Begun, G. M.; Peiffert, C.; Mesmer, R. E. *J. Solution Chem.* **2000**, *29*, 101. (b) Nguyen-Trung, C.; Begun, G. M.; Palmer, D. A. *Inorg. Chem.* **1992**, *31*, 5280. (c) Sarsfield, M. J.; Helliwell, M.; Raftery, J. *Inorg. Chem.* **2004**, *43*, 3170. (d) Oda, Y.; Aoshima, A. *J. Nucl. Sci. Technol.* **2002**, *39*, 647.

(28) Danis, J. A.; Lin, M. R.; Scott, B. L.; Eichhorn, B. W.; Runde, W. H. *Inorg. Chem.* **2001**, *40*, 3389.

(29) Smirnov, M. V. *Electrode Potentials in Molten Chlorides*; Nauka: Moscow, 1973.

(30) (a) Kuznetsov, S. A.; Hayashi, H.; Minato, K.; Gaune-Escard, M. *J. Electrochem. Soc.* **2005**, *152*, C203. (b) Nekrasova, N. P.; Komarov, V. E. *Radiokhimiya* **1983**, *25*, 233.

(31) Riglet, Ch.; Vitorge, P.; Grenthe, I. *Inorg. Chim. Acta* **1987**, *133*, 323.

(32) Deuber, R. E.; Bond, A. M.; Dickens, P. G. *J. Electrochem. Soc.* **1994**, *141*, 311.

(33) Cherginets, V. L.; Demirskaya, O. V.; Rebrova, T. P. *J. Chem. Thermodyn.* **2004**, *36*, 115.

(34) (a) Crosswhite, H. M.; Crosswhite, H.; Carnall, W. T.; Paszek, A. P. *J. Chem. Phys.* **1980**, *72*, 5103. (b) Schelter, E. J.; Yang, P.; Scott, B. L.; Thompson, J. D.; Martin, R. L.; Hay, P. J.; Morris, D. E.; Kiplinger, J. L. *Inorg. Chem.* **2007**, *46*, 7477.

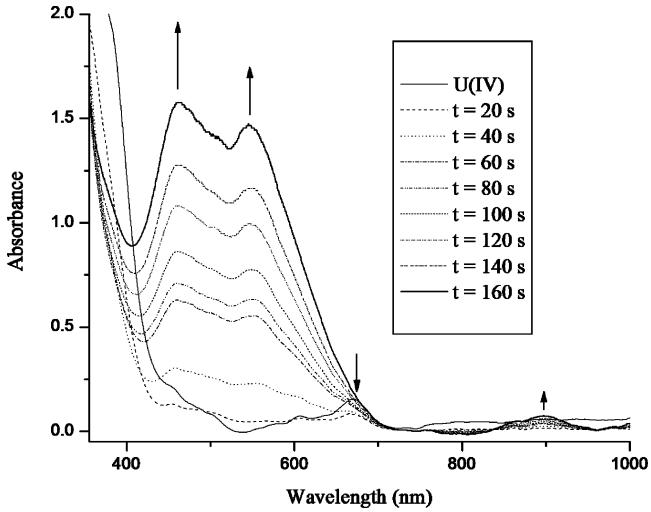

Figure 4. In situ EAS spectra at various time intervals from the electrochemical reduction of uranium(IV) to uranium(III) by chronopotentiometry at 15 mA in a LiCl−KCl eutectic at 450 °C.

uranium(III) quickly evolved. The chemical reduction of $[UCl_6]^{2-}$ with uranium metal confirms the results from our previous EAS investigations that even a small fraction of uranium(III) can swamp the absorbances for uranium(IV). Monitoring of the potential during the electrochemical reduction of uranium(IV) to uranium(III) in a molten LiCl−KCl eutectic indicated a very slow rate of reduction and was still incomplete after 4 h of electrolysis. However, the anodic dissolution of uranium, monitored by EAS, produced a pure uranium(III)-containing melt, as proven by oxidimetric analysis of the subsequent quenched melt.

In Situ XAS Spectroelectrochemistry. We have further developed our specially adapted furnace for XAS measurements for fluorescence detection by incorporating beryllium windows at 90° angles to one another (Figure 1). This not only has increased the sensitivity of the XAS signal obtained in high-temperature systems but also opened the possibility of speciating in high-X-ray-absorbing melts containing heavier alkali metals (e.g., K^+, Cs^+). Thus, concentrations of less than millimolar levels, where conventional electrochemistry is predominantly performed, could be assessed. This EXAFS technique has been applied to the investigation of high-specific-activity nuclides in an aqueous solution.[35] Fluorescence detection has been used to study the X-ray absorption near-edge structure (XANES) region in order to determine the formal potentials of neptunium redox couples.[36]

Anodic dissolution of uranium to give a single soluble species was performed to validate our method. The EXAFS spectrum obtained (Figure 5) was fitted with a single shell of six chlorine atoms at 2.83 ± 0.02 Å (Table 4). Subsequent analysis of the quenched melt showed that the final melt contained 2.21 wt % uranium with an

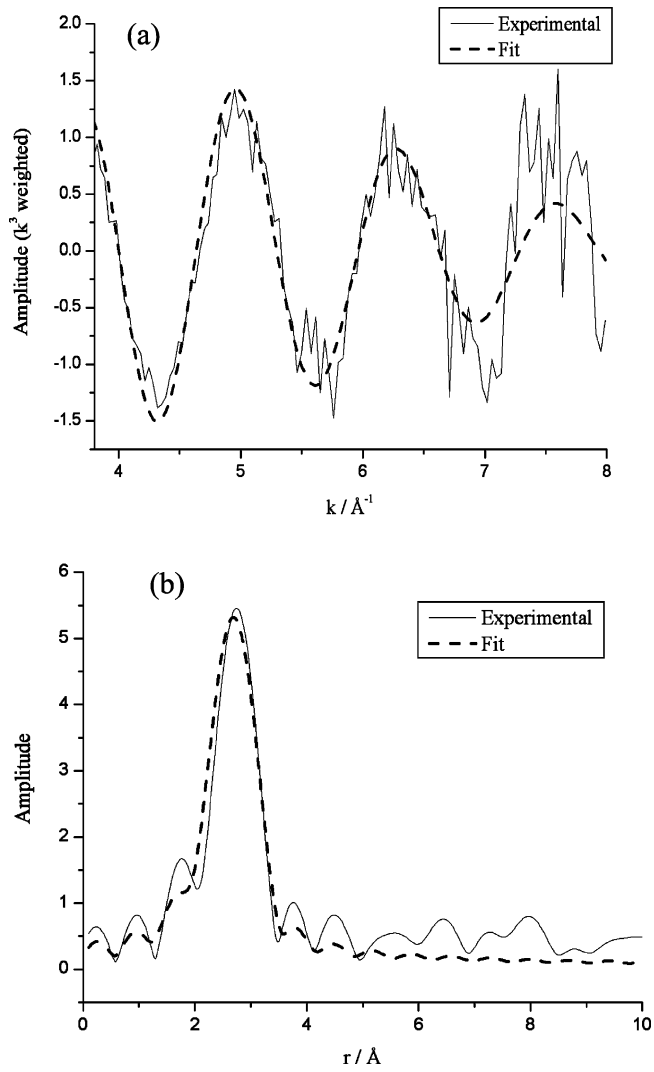

Figure 5. U L_{III}-edge EXAFS spectrum of uranium anodic dissolution in a LiCl−KCl eutectic at 450 °C (a) with Fourier transformation (b).

average oxidation state of 3.14 (±5%). We believe a value slightly above 3 is obtained because of oxidation during analysis. The U−Cl distance is comparable to that obtained by Okamoto et al. (2.82 ± 0.01 Å) for UCl_3 dissolved in a LiCl−KCl eutectic (15 wt % U) at 600 °C[7] and is significantly larger than U^{IV}−Cl distances obtained in both high-temperature alkali chloride melts (2.62−2.69 Å)[10,11] and for $[UCl_6]^{2-}$ in solid-state structures (2.55−2.70 Å).[37] These results are consistent with the formation of $[UCl_6]^{3-}$ and not the production of uranium(IV). No other shells were included in the model because of the high levels of noise in the high-*k* region of the spectrum, with the most likely cause being the walls of the quartz cell absorbing much of the fluorescence emitted. Therefore, electrochemical dissolution pro-

(35) Antonio, M. R.; Soderholm, L.; Williams, C. W.; Blaudeau, J.-P.; Bursten, B. E. *Radiochim. Acta* **2001**, *89*, 17.

(36) Soderholm, L.; Antonio, M. R.; Williams, C.; Wasserman, S. R. *Anal. Chem.* **1999**, *71*, 4622.

(37) (a) de Villardi, G. C.; Charpin, P.; Costes, R.-M.; Folcher, G.; Plurien, P.; Rigny, P.; de Rango, C. *Chem. Commun.* **1978**, 90. (b) Rogers, R. D.; Kurihara, L. K.; Benning, M. M. *Inorg. Chem.* **1984**, *121*, 168. (c) Charpin, P.; Lance, M.; Nierlich, M.; Vigner, D.; Marquet-Ellis, H. *Acta Crystallogr. C* **1988**, *44*, 257.

Table 4. EXAFS Data of Uranium(III) Species

sample	[U] (wt %)	k_{max},(Å^{-1})	occupancy[b]	distance (Å)[c]	$2\sigma^2$ (Å^2)[d]	*R*
UCl_3 in LiCl at 750 °C[a]	10.3	10	U−O(0.5)	1.69	0.011	27.9
			U−Cl(6)	2.72	0.050	
			U−Li(12)	3.26	0.057	
UCl_3 in LiCl, quenched[a]	10.3	11	U−Cl(6)	2.91	0.014	28.9
anodic dissolution of uranium metal in a LiCl−KCl eutectic at 450 °C	2.21	8.0	U−Cl(6)	2.83	0.053	37.2

[a] Reference 9. [b] ±20%. [c] ±0.02 Å. [d] $2\sigma^2$ = Debye−Waller factor.

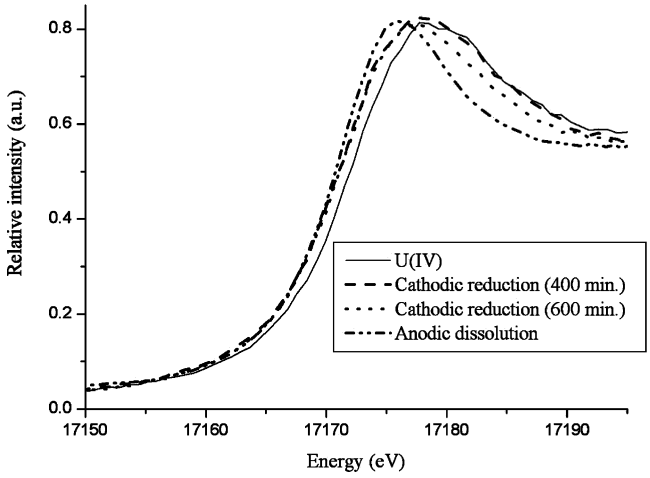

Figure 6. U L_{III}-edge XAS spectra of uranium cathodic reduction ($U^{IV} \rightarrow U^{III}$) and anodic dissolution (U metal $\rightarrow U^{III}$) in LiCl−KCl at 450 °C.

vides an ideal method for monitoring pure uranium(III) in high-temperature melts because the influence of external factors, such as oxygen contamination, are minimized.

Cathodic reduction of uranium(IV) to uranium(III) was performed to investigate whether our spectroelectrochemical method could be used to monitor the progress of reactions in high-temperature melts. It was observed that the initial green melt had changed color to a deep purple with the application of the reducing potential. Analysis of the XANES region indicated that there was a negative shift in the U L_{III}-edge position[38] after 400 min of electrolysis (Figure 6), which would be expected with the conversion of uranium(IV) to uranium(III), although the magnitude of the shift was only 1 eV, from 17 172.3 to 17 171.3 eV. This is probably indicative of incomplete reduction because typically a difference of over 3 eV was observed for uranium(IV) vs uranium(III) XANES edge positions.[7] The equivalent EAS spectroelectrochemical experiments also showed that complete reduction of uranium(IV) to uranium(III) in chloride melts is extremely difficult to achieve. The EXAFS results indicate the expected increase in the U−Cl distance of the first coordination shell with the reduction process, although the fits obtained are poor because of the high levels of noise present.

The XANES region of the anodic dissolution experiments show a 1.3 eV negative shift in the U L_{III}-edge position relative to that for the initial uranium(IV) scans from the cathodic reduction experiments (Figure 6). The absorption edge for the anodic dissolution melt was found at 17 171.0 eV. The U L_{III}-edge position for solid UCl_3 (mixed in boron nitride) was observed at 17 169 eV, and previously reported absorption edges for various solid uranium(III) compounds range between 17 170 and 17 173 eV.[39] The absorption edge for $[UCl_6]^{2-}$ in a molten LiCl−KCl eutectic was found at 17 172.3 eV, while the edge for various solid uranium(IV) compounds is known to fall between 17 173 and 17 177 eV.[39] Oxidimetric analysis of the quenched melts produced in the equivalent EAS spectroelectrochemical experiments provides the most definitive evidence that anodic dissolution is the most efficient method for electrolytically generating uranium(III) in a molten LiCl−KCl eutectic. We believe that the poor efficiency of the reduction process is predominantly due to the diffusion properties of the molten salt in conjunction with the shape of the cell required for these measurements. The electroreduction of uranium(IV) to uranium(III) in room temperature ionic liquids is also seen to be difficult to force to completion and in this case is attributed to the presence of oxides and protons in the solvent, which reoxidize some of the uranium(III) back to uranium(IV).[40] A similar process may occur in our high-temperature systems.

Conclusions

Monitoring of uranium speciation and redox processes in high-temperature alkali metal chloride melts poses a number of technical challenges. However, we have now reached the stage where we can use XAS and EAS spectroscopy to investigate this system across a series of uranium oxidation states (III, IV, V, and VI). We can also apply spectroelectrochemical methods to study redox processes, including the anodic dissolution of uranium metal to uranium(III), an industrially very significant process. However, while EXAFS spectroscopy points to the presence of a longer range ordering of uranium species in chloride melts (beyond simple anionic chloride and oxychloride species), it is difficult to obtain more detail about the extended structures that may be present. In addition, the strong absorption of uranium(III) in the visible region inhibits the use of EAS to probe other uranium oxidation states in the presence of significant quantities of this trivalent species, which will dominate process speciation. Clearly, additional, comple-

(38) The edge position was determined by the maximum of the first derivative of the XAS raw data. The values quoted have an estimated error of ±0.5 eV.

mentary in situ spectroscopic tools need to be developed, including more advanced XAS techniques and Raman spectroscopy.

Acknowledgment. We thank Nexia Solutions for financial support (to C.A.S. and V.A.V.) and INTAS for a fellowship (to I.B.P.).

Supporting Information Available: Listings of fitted absorption spectra and absorption data plots. This material is available free of charge via the Internet at http://pubs.acs.org.

IC701415Z

(39) (a) Akiyama, K.; Sueki, K.; Haba, H.; Tsukada, K.; Asai, M.; Yaita, T.; Nagame, Y.; Kikuchi, K.; Katada, M.; Nakahara, H. *J. Radioanal. Nucl. Chem.* **2003**, *255*, 15. (b) Kalkowski, G.; Kaindle, G.; Brewer, W. D.; Krone, W. *Phys. Rev. B* **1987**, *35*, 2667. (c) Hu, Z.; Kaindle, G.; Meyer, G. *J. Alloys Compd.* **1998**, *274*, 38. (d) Docrat, T. I.; Mosselmans, J. F. W.; Charnock, J. M.; Whiteley, M. W.; Collison, D.; Livens, F. R.; Jones, C.; Edminston, M. J. *Inorg. Chem.* **1999**, *38*, 1879.

(40) Anderson, C. J.; Deakin, M. R.; Choppin, G. R.; D'Olienslager, W.; Heerman, L.; Pruett, D. J. *Inorg. Chem.* **1991**, *30*, 4013.